Millimeter/Submillimeter-Wave Spectrum of the VCl+ Radical in its X 4Σ− Ground State†

ARTICLE *in* THE JOURNAL OF PHYSICAL CHEMISTRY A · NOVEMBER 2009

Impact Factor: 2.69 · DOI: 10.1021/jp9058142 · Source: PubMed

2 AUTHORS, INCLUDING:

Dewayne Terrence Halfen
The University of Arizona
102 PUBLICATIONS **548** CITATIONS

Millimeter/Submillimeter-Wave Spectrum of the VCl^+ Radical in its X $^4\Sigma^-$ Ground State†

D. T. Halfen* and L. M. Ziurys

Department of Chemistry, Department of Astronomy, Arizona Radio Observatory, and Steward Observatory, University of Arizona, 933 N. Cherry Avenue, Tucson, Arizona 85721

Received: June 20, 2009; Revised Manuscript Received: August 17, 2009

The pure rotational spectrum of the molecular ion VCl^+ (X $^4\Sigma^-$) has been recorded from 274 to 419 GHz using a combination of millimeter direct absorption and velocity modulation spectroscopy. This study is the first spectroscopic measurement of this species in the laboratory, which has also enabled the determination of the ground state term, $^4\Sigma^-$. VCl^+ was produced in an AC discharge of VCl_4 and argon. Fifteen and eleven rotational transitions were recorded for the $V^{35}Cl^+$ and $V^{37}Cl^+$ isotopologues, respectively. The fine structure splittings of the $^4\Sigma^-$ state were found to deviate significantly from a case (b) pattern. Specifically, spin components from adjacent rotational transitions were found to overlap in frequency. Unusual vanadium hyperfine splittings were also observed in the VCl^+ spectra; the expected vanadium octet was clearly present for the F_2 and F_3 spin components but was partially collapsed and reversed in frequency ordering in the F_1 and F_4 cases. The data were analyzed in a global fit, and rotational, fine structure, and hyperfine constants were determined. For VCl^+, the values of both the spin−spin and spin-rotation parameters are extremely large, as were the third-order hyperfine and spin-rotation terms, b_s and γ_s. For example, the spin−spin constant is $\lambda = 417\,900(22\,700)$ MHz, while $\gamma = 6567(51)$ MHz. The values of these constants indicate a high density of excited electronic states close to the ground state, which contribute to second and third-order spin−orbit coupling. The hyperfine constants suggest a $\sigma^1\pi^2$ electron configuration, as opposed to $\sigma^1\delta^2$, as found in VS and VO. The bond length of VCl^+, $r_0 = 2.119(2)$ Å, is shorter than that of VCl by 0.1 Å, which has $r_0 = 2.219$ Å. The decrease in bond length is attributed to an increase in the electrostatic attraction between V^{2+} and Cl^-, as opposed to V^+ and Cl^- for VCl.

1. Introduction

Although small, neutral transition metal-bearing species have been the subject of numerous spectroscopic studies across many wavelength regions,[1−13] few ionic molecules of this type have been investigated at high resolution. This situation is likely a consequence of the difficulties in creating molecular ions, particularly those with a refractory metal atom. Among the few that have been investigated are TiF^+, $TiCl^+$, FeO^+, and $FeCO^+$. These species have been studied via their electronic or vibrational transitions at optical and infrared wavelengths.[14−17] The millimeter/submillimeter spectrum of all four molecular ions has recently been measured as well by Halfen and Ziurys, using direct absorption combined with velocity modulation techniques.[18−21]

Another transition metal-bearing molecular ion of interest is VCl^+. While previous experimental work of this species does not exist, there is a recent theoretical study by Kardahakis and Mavridis.[22] These authors predicted the ground electronic state to be $^4\Pi$, with $^4\Sigma$ also being a possibility.[22] The neutral counterpart VCl has a $^5\Delta_r$ ground state originating from an electron configuration of (core)$11\sigma^1 1\delta^1 5\pi^2$, based on calculations by Ram et al.,[2] and recently confirmed by rotational measurements of Halfen, Brown, and Ziurys.[3] TiCl and VS are both isoelectronic with VCl^+, and their ground states are X $^4\Phi_r$ and X $^4\Sigma^-$, respectively, with electron configurations of (core)$11\sigma^1 1\delta^1 5\pi^1$ and (core)$11\sigma^1 1\delta^2$.[4,5] An X $^4\Pi$ state for VCl^+, as suggested by theory, would result from a (core)$1\delta^2 5\pi^1$ configuration, requiring significant rearrangement of electrons from the configuration of VCl. Removal of the δ electron would produce the $^4\Sigma^-$ state. High resolution spectroscopy of VCl^+ would certainly aid in establishing the correct ground state term for this molecular ion.

Here we report the first laboratory detection of VCl^+ in its ground electronic state and measurement of its pure rotational spectrum. Four spin components of equal intensity were observed for both the $^{51}V^{35}Cl^+$ and $^{51}V^{37}Cl^+$ isotopologues, the signature of a $^4\Sigma$ ground state. No evidence of λ-doubling was found, as expected for a Π state. The data have been analyzed and spectroscopic constants determined. The parameters indicate that excited electronic states lie close in energy, as suggested by theory. Here we present our results, analysis, and interpretation of the fine and hyperfine terms.

2. Experimental Section

The pure rotational spectrum of the VCl^+ radical was measured using a millimeter/submillimeter velocity modulation system. This instrument consists of a radiation source, free-space gas cell, and detector and has been described in detail elsewhere.[23] The frequency source is a Gunn oscillator/Schottky multiplier combination that operates between 65 and 850 GHz. The reaction vessel is a glass cell 4 in. in diameter and 32 in. in length containing two ring electrodes that create a longitudinal AC discharge. The cell is surrounded by a cooling jacket, chilled to −65 °C with methanol. The detector is an InSb hot electron bolometer. The instrument can be employed as a classic direct absorption system with FM modulation of the source. Alternately, the AC discharge can be used to velocity modulate ionic species.[19,23] Source modulation is normally used for initial, broad

† Part of the "Robert W. Field Festschrift".

* Phone: 520-626-0701. Fax: 520-621-5554. E-mail: halfendt@as.arizona.edu.

10.1021/jp9058142 CCC: $40.75
Published on Web 09/11/2009

searches; velocity modulation is employed to discriminate ion from neutral signals.

VCl^+ was produced in an AC discharge (250 W with 600 Ω at 20 kHz) of less than 1 mTorr of gas-phase VCl_4 and 30−40 mTorr of argon. The plasma glowed a dark purple color when adding the reactant materials; however, this glow was quickly obscured by purple-black residue coating the inside of the gas cell. ***Caution!*** *Care should be taken with handling VCl_4, as it is extremely toxic and corrosive.*

Transitions of VCl^+ were found by continuously scanning the region 360−400 GHz in 100 MHz increments. Numerous lines of neutral VCl were seen in the course of these measurements; these data have been analyzed and presented elsewhere.[3] The remaining spectral features arose from a species with a significantly larger rotational constant, 5427.1 vs 4949.8 MHz. The presence of octets indicated that the molecule contained vanadium, which has a nuclear spin of $I = {}^7/_2$. The pattern also repeated in what appeared to be ^{35}Cl and ^{37}Cl isotopes, indicating the presence of chlorine in the species. Use of velocity modulation confirmed that the lines arose from an ionic species, identified as VCl^+.

Precise rest frequencies were determined by averaging pairs of 5 MHz wide scans, one increasing and the other decreasing in frequency. Typically 6−16 scan pairs were needed to achieve a sufficient signal-to-noise ratio. Transition frequencies and line widths were determined by fitting Gaussian profiles to the spectral features. The line widths varied from 900 kHz at 274 GHz to 1500 kHz at 419 GHz. The experimental error is estimated to be ± 50 kHz.

3. Results

The spectral pattern exhibited by VCl^+ at first seemed simple to assign. A series of "quartets" were observed spaced by ∼11 GHz. Based on VCl, the rotational constant of VCl^+ was estimated to be near ∼5 GHz, in good agreement with the observed spectra. It was first thought that VCl^+ exhibited a classic Hund's case (b) pattern, as seen for CrN.[6] However, the quartet pattern turned out to be an accidental coincidence. The "quartet" was actually two separate spin components from two adjacent rotational transitions: F_3 and F_4 from $N + 2 \leftarrow N + 1$ and F_1 and F_2 from $N + 1 \leftarrow N$.

The observed pattern for VCl^+ is illustrated in Figure 1, which displays a stick spectrum of one rotational transition, $N = 32 \leftarrow 31$ (solid lines), and parts of two others that fall in the same frequency range, $N = 31 \leftarrow 30$ and $N = 33 \leftarrow 32$ (dashed and dot-dashed lines, respectively). The pseudo "quartet" is located within a 4 GHz range, with the first two fine structure components belonging to the $N + 2 \leftarrow N + 1$ transition and the next two features to $N + 1 \leftarrow N$. The F_4, F_3, F_2, and F_1 spin components of the $N = 32 \leftarrow 31$ transition, the "true" quartet, are spaced across ∼16 GHz. (F_1 corresponds to $J = N + 3/2$, F_2 is $J = N + 1/2$, etc.) The four spin components have very similar intensities and are single features, ruling out a $^4\Pi$, $^4\Delta$, or $^4\Phi$ state. For a regular ground state with $\Lambda \neq 0$, the relative intensities for the fine structure components would decrease with increasing Ω, and lambda-doubling would likely be present, as well.

The hyperfine pattern, arising from the vanadium spin of $I(^{51}V) = {}^7/_2$, exhibited some unusual effects. Vanadium nuclear coupling often produces a distinct octet pattern, as found in VN.[8] The F_2 and F_3 spin components display this expected pattern, with a total splitting of 15−18 MHz across the octet. The hyperfine structure of the F_1 and F_4 components, on the other hand, is not completely resolved into eight distinct features. The higher F transitions for the F_1 spin component and the lower F transitions of the F_4 component are collapsed into one line; the overall hyperfine splitting is therefore 7−9 MHz wide. The ordering of the hyperfine components is also reversed for the F_1 and F_4 lines vs the F_2 and F_3 features. The high $F' \leftarrow F''$ transitions are at higher frequency for the F_1 and F_4 components but appear at lower frequency for the F_2 and F_3 components. The details of the F ordering can be seen in Figure 2 and Table 1.

Figure 2 shows a representative spectrum of the "quartet" of VCl^+. Here two spin components from two different rotational

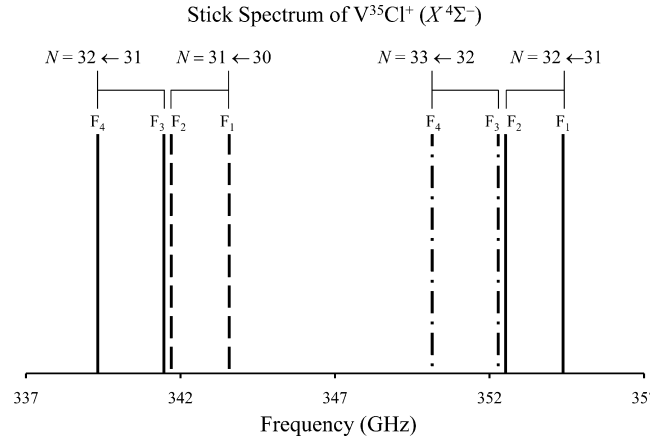

Figure 1. Stick spectrum of the spin quartet of the $N = 32 \leftarrow 31$ rotational transition of $V^{35}Cl^+$, along with the interloping spin components of the $N = 31 \leftarrow 30$ and $N = 33 \leftarrow 32$ transitions, in the range 337−357 GHz. The overall fine structure splitting per transitions is ∼16 GHz, with the F_3 and F_4 components toward lower frequency, and the F_1 and F_2 components located at the higher end. The hyperfine splittings are too small to show on the given scale; hence, the relative intensities of the spin components have been are averaged over the hyperfine lines. The figure illustrates that VCl^+ has a Hund's case (a) coupling scheme.

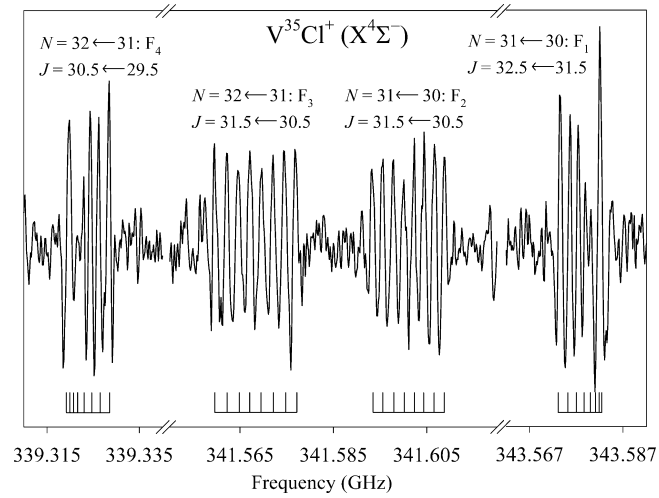

Figure 2. Representative spectrum of VCl^+ ($X\,^4\Sigma^-$) near 340 GHz, which consists of two fine structure components each from the rotational transitions $N = 31 \leftarrow 30$ and $32 \leftarrow 31$. There are two frequency gaps in the spectrum to show the two sets of spin components, which are displayed on the same intensity scale. Each component is split by vanadium hyperfine interactions. The frequencies of the hyperfine components are shown underneath the spectrum (also see Table 1). The F_2 and F_3 spin components display an evenly spaced octet; the F_1 and F_4 components have blended features. This spectrum was created from three separate, 110 MHz wide, scan averages, each consisting of four 70 s subscans, and then cropped to display 30, 70, and 30 MHz frequency ranges, respectively.

TABLE 1: Selected Rotational Transitions of VCl^+ ($X\ ^4\Sigma^-$)[a]

									$V^{35}Cl^+$		$V^{37}Cl^+$	
N'	←	N''	J'	←	J''	F'	←	F''	ν_{obs}	$\nu_{obs} - \nu_{calc}$	ν_{obs}	$\nu_{obs} - \nu_{calc}$
33	←	32	31.5	←	30.5	28	←	27	350141.717	0.257	338980.600	−0.027
						29	←	28	350141.717	0.029	338980.600	0.101
						30	←	29	350141.717	−0.637	338980.600	−0.362
						31	←	30	350143.670	0.265	338982.247	0.318
						32	←	31	350144.881	0.096	338983.726	0.415
						33	←	32	350146.489	0.053	338985.215	0.207
						34	←	33	350148.206	−0.087	338986.772	−0.147
						35	←	34	350150.284	−0.004	338988.568	−0.362
33	←	32	32.5	←	31.5	29	←	28	352392.121	0.131	341190.554	0.091
						30	←	29	352389.705	0.224	341188.040	0.127
						31	←	30	352387.203	0.125	341185.657	0.102
						32	←	31	352384.716	−0.018	341183.095	−0.210
						33	←	32	352382.233	−0.162	341180.867	−0.209
						34	←	33	352379.778	−0.229	341178.477	−0.295
						35	←	34	352377.249	−0.263	341176.295	0.001
						36	←	35	352375.052	0.206	*b*	
33	←	32	33.5	←	32.5	30	←	29	363241.676	−0.021	351693.639	−0.027
						31	←	30	363239.486	0.102	351691.513	0.186
						32	←	31	363237.374	0.189	351689.276	0.094
						33	←	32	363235.544	0.487	351687.223	0.070
						34	←	33	363233.138	0.185	351685.229	0.071
						35	←	34	363230.733	−0.086	351682.936	−0.172
						36	←	35	363228.334	−0.270	351680.816	−0.094
						37	←	36	363225.833	−0.416	351678.778	0.313
33	←	32	34.5	←	33.5	31	←	30	365180.873	−0.090	353550.816	0.128
						32	←	31	365182.831	−0.010	353552.523	−0.071
						33	←	32	365184.564	−0.021	353554.260	−0.138
						34	←	33	365186.087	−0.065	353555.836	−0.187
						35	←	34	365187.571	0.074	353557.176	−0.212
						36	←	35	365188.921	0.348	353558.765	0.360
						37	←	36	365189.469	0.139	353558.765	−0.215
						38	←	37	365189.469	−0.245	353558.765	−0.253
34	←	33	32.5	←	31.5	29	←	28	360961.790	0.338	349456.741	0.268
						30	←	29	360961.790	0.003	349456.741	0.274
						31	←	30	360961.790	−0.732	349456.741	−0.265
						32	←	31	360963.640	0.034	349457.519	−0.492
						33	←	32	360965.066	0.081	349459.538	0.146
						34	←	33	360966.578	−0.024	349461.108	0.050
						35	←	34	360968.396	0.000	349462.869	−0.039
						36	←	35	360970.366	0.066	349464.759	−0.079
34	←	33	33.5	←	32.5	30	←	29	363204.996	0.085	351660.526	−0.026
						31	←	30	363202.568	0.180	351658.190	0.180
						32	←	31	363200.072	0.107	351655.841	0.192
						33	←	32	363197.659	0.062	351653.386	−0.006
						34	←	33	363195.122	−0.113	351651.084	−0.069
						35	←	34	363192.605	−0.221	351648.662	−0.183
						36	←	35	363190.126	−0.189	351646.246	−0.126
						37	←	36	363187.660	0.016	351643.917	0.283
34	←	33	34.5	←	33.5	31	←	30	374054.386	−0.141	362163.379	−0.221
						32	←	31	374052.197	−0.009	362161.342	0.068
						33	←	32	374050.093	0.096	362159.098	−0.035
						34	←	33	374047.915	0.058	362156.834	−0.271
						35	←	34	374045.684	−0.056	*b*	
						36	←	35	374043.511	−0.089	*b*	
						37	←	36	374041.237	−0.147	*b*	
						38	←	37	374039.147	0.107	*b*	
34	←	33	35.5	←	34.5	32	←	31	375980.501	−0.205	*b*	
						33	←	32	375982.511	0.008	*b*	
						34	←	33	375984.264	0.077	*b*	
						35	←	34	375985.664	−0.056	*b*	
						36	←	35	375987.076	0.015	*b*	
						37	←	36	375988.135	−0.032	*b*	
						38	←	37	375989.115	0.123	*b*	
						39	←	38	375989.115	−0.371	*b*	

[a] In MHz, for $v = 0$. [b] Blended lines. Not included in fit.

transitions, $N = 31 \leftarrow 30$ and $N = 32 \leftarrow 31$, are shown, labeled by N and J. There are two frequency breaks in the figure. The positions of the vanadium hyperfine components are indicated underneath the data. The octet pattern is clearly apparent for

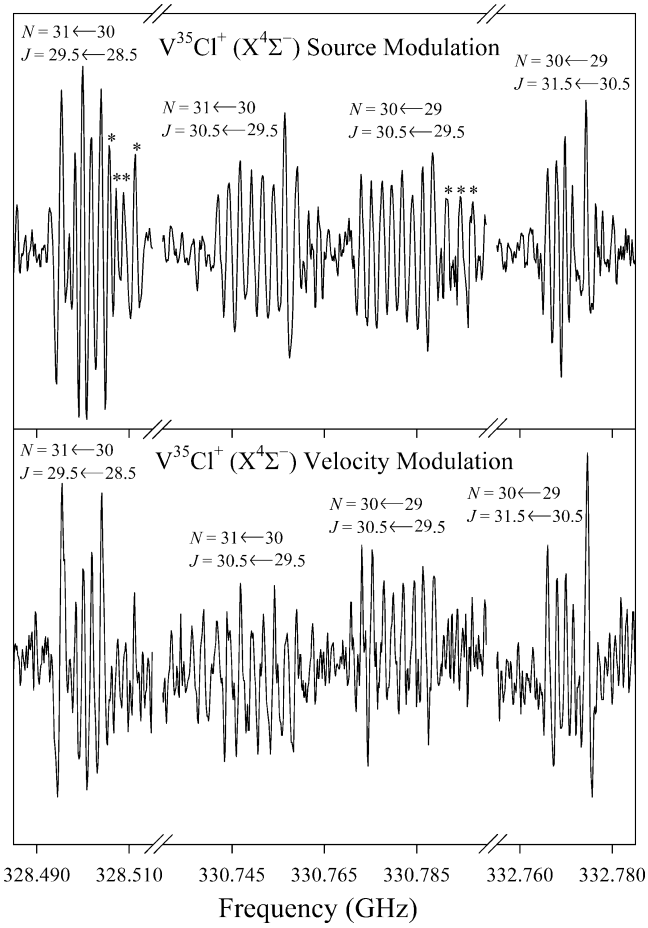

Figure 3. Spectra of VCl^+ taken using source modulation (upper panel) and velocity modulation (lower panel). Two fine structure components from two rotational transitions are displayed in these data, similar to Figure 2. Two spin components ($J = 30.5 \leftarrow 29.5$, $N = 30 \leftarrow 29$ and $J = 29.5 \leftarrow 28.5$, $N = 31 \leftarrow 30$ transitions) are partially blended with lines from the neutral species, VCl, indicated in the data by stars (upper panel). These features disappear in velocity modulation mode, leaving behind only features from VCl^+ (lower panel). The difference in the signal intensity between source and velocity modulation is about a factor of 4.

the F_2 and F_3 spin components. The F_1 and F_4 hyperfine lines do not exhibit this regular pattern and certain features appear stronger in the spectrum only because they are multiple blended components. The $V^{37}Cl^+$ spectrum appears to be similar, but the intensity is less by a factor of 3 due to the lower ^{37}Cl natural abundance (^{35}Cl:$^{37}Cl = 75.4$:24.6).

Table 1 lists selected rotational transitions measured for the $V^{35}Cl^+$ and $V^{37}Cl^+$ isotopologues. Fifteen and eleven rotational transitions were recorded for $V^{35}Cl^+$ and $V^{37}Cl^+$, respectively, and the complete data set is available in the Supporting Information. As seen in the table, the hyperfine structure varies for the individual spin components.

Figure 3 presents concrete evidence that the assigned features are due to an ionic species. Here the "quartet" attributed to the $N = 30 \leftarrow 29$ and $N = 31 \leftarrow 30$ transitions of VCl^+ are shown. The upper panel displays the spectrum in source modulation mode, with second derivative profiles. Several neutral interloper lines are marked by stars, arising from what is likely to be vibrationally excited VCl. The same spectrum of VCl^+ taken in velocity modulation mode is shown in the lower panel, with first-derivative line profiles in this case. The "quartet" in question is still present in these data, but the neutral interloping features have disappeared. The signal intensity is a factor of ~4 lower in these data, however, due to undermodulation of the lines.

TABLE 2: Spectroscopic Constants for VCl^+ ($X\ ^4\Sigma^-$: $v = 0$)[a]

parameter	$V^{35}Cl^+$	$V^{37}Cl^+$
B	5427.1033(30)	5254.1688(66)
D	0.0032037(13)	0.0030017(24)
γ	6567(51)	6404(77)
γ_D	−0.04876(53)	−0.0453(13)
γ_H	$-3.1(1.5) \times 10^{-7}$	$-3.8(3.2) \times 10^{-7}$
γ_s	1436(51)	1406(26)
λ	417900(22700)	396300(34900)
λ_D	0.162(30)	0.298(46)
λ_H	$-7.10(44) \times 10^{-5}$	$-7.16(16) \times 10^{-5}$
λ_L	$-2.1(1.4) \times 10^{-9}$	
b_F	138(14)	184(28)
c	341(63)	485(130)
b_{FD}	−0.580(18)	−0.537(25)
c_D	−1.651(41)	−1.539(56)
b_s	−96.1(7.6)	−102(12)
b_{sD}	−0.0092(28)	−0.0072(45)
C_I	2.323(92)	2.25(12)
eQq	−560(180)	−950(320)
rms of fit	0.206	0.205
r_0 (Å)	2.119173(2)	2.118988(4)

[a] In MHz; errors are 3σ in the last quoted decimal places.

4. Analysis

In a $^4\Sigma$ state, the separation between the rotationless $|\Sigma|$ components is given by 4λ, and therefore this parameter plays a similar role as the spin−orbit constant in states with $\Lambda \neq 0$.[10] For heavily perturbed $^4\Sigma$ states, the upper $+\Sigma$ ladder ($\Sigma = {}^3/_2$) may be easily distinguished by the relative inability of the **S**-uncoupling operator to distort the rotational progression compared with the lower $-\Sigma$ ladder. For a few trial values of γ ($\gamma \ll \lambda$), λ (and λ_D) can be established by fitting the $\Sigma = {}^3/_2$ spin levels. This estimate for λ leads to the assignment of the $\Sigma = {}^1/_2$ doublet. This initial process for VCl^+ yielded a value for λ of approximately 420 GHz, which results in a rotationless splitting of the $|\Sigma|$ components of 55 cm^{-1}. This method enabled the assignment of the four lines of the "pseudo" quartet as transitions involving $J - 1 \leftarrow J-2$, $J \leftarrow J - 1$, $J \leftarrow J - 1$, and $J + 1 \leftarrow J$. This result meant that the "quartet" actually involved two rotational transitions, $N + 2 \leftarrow N + 1$ and $N + 1 \leftarrow N$, in case b notation.

Once the identity of the "quartet" was established, the spectrum of VCl^+ could then be analyzed with an effective Hund's case (b) Hamiltonian.[24] This Hamiltonian consists of rotational, spin-rotation, third-order spin-rotation,[25] spin−spin, magnetic hyperfine, third-order magnetic hyperfine,[26] nuclear spin-rotation, and electric quadrupole interactions:

$$\hat{H}_{\mathrm{eff}} = \hat{H}_{\mathrm{rot}} + \hat{H}_{\mathrm{sr}} + \hat{H}^{(3)}_{\mathrm{sr}} + \hat{H}_{\mathrm{ss}} + \hat{H}_{\mathrm{mhf}} + \hat{H}^{(3)}_{\mathrm{mhf}} + \hat{H}_{\mathrm{nsr}} + \hat{H}_{\mathrm{eQq}} \quad (1)$$

A global fit was performed of the $V^{35}Cl^+$ and $V^{37}Cl^+$ data sets separately, and the resulting spectroscopic constants are listed in Table 2. The third-order terms in spin-rotation $\hat{H}^{(3)}_{\mathrm{sr}}$ and magnetic hyperfine $\hat{H}^{(3)}_{\mathrm{mhf}}$ were necessary to achieve an acceptable rms value, along with the higher-order centrifugal distortion parameters γ_H, λ_H, and λ_L. Immediately obvious from the table is that γ and λ are large and greater than the rotational constant B. In addition, γ_s is only a factor of ~5 times smaller than γ. These parameter values indicate that the molecule has a high

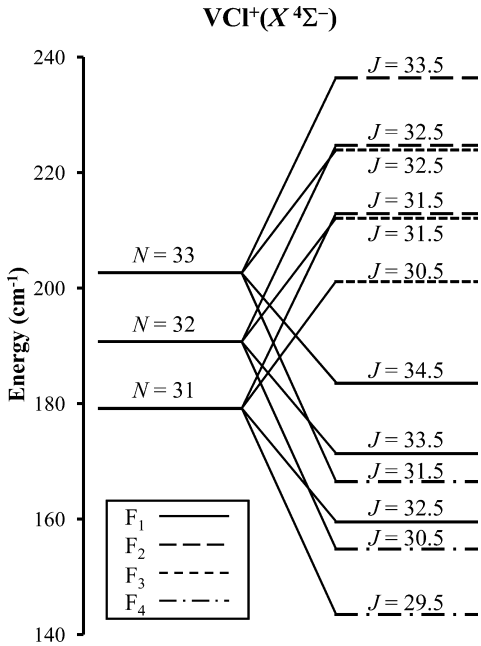

Figure 4. Energy level diagram of VCl^+ showing the $N = 31$, 32, and 33 rotational levels. Each state is split into four fine structure components, indicated by the different line types. The fine structure levels are separated into effective Ω ladders with F_1 and F_4 corresponding to $\Omega = \pm^1/_2$ and F_2 and F_3 as $\Omega = \pm^3/_2$.

degree of second-order spin−orbit coupling and is rapidly progressing toward Hund's case (a). This evolution is also evident in the third-order hyperfine constant b_s, which is the same order of magnitude as b_F, the Fermi contact term. The electric quadrupole coupling constant eQq for $V^{35}Cl^+$ and $V^{37}Cl^+$ are −560(180) and −950(320) MHz, respectively. These parameters have large errors and are essentially the same within the experimental uncertainty.

5. Discussion

The ground state of VCl^+ has been determined to be $^4\Sigma^-$. The only theoretical work on this ion suggests that this term is quite possible.[22] Elimination of one electron from VCl, which has an electron configuration of (core)$11\sigma^1 1\delta^1 5\pi^2$ ($^5\Delta_r$),[3] can lead to several electronic terms. Studies of $TiCl^+$, $FeCO^+$, and FeO^+ by our group and others suggest that the ion is usually produced by removal of an electron from a single orbital of the neutral without additional rearrangement of the configuration.[19−21] For example, TiCl, FeCO, and FeO have ground state configurations of (core)$11\sigma^1 1\delta^1 5\pi^1$ ($^4\Phi_r$), (core)$4\pi^4 11\sigma^2 1\delta^2$ ($^3\Sigma^-$), and (core)$9\sigma^1 1\delta^3 4\pi^2$ ($^5\Delta_i$).[4,7,8] Their positive ions $TiCl^+$, $FeCO^+$, and FeO^+ have configurations of (core)$1\delta^1 5\pi^1$ ($^3\Phi_r$), (core)$4\pi^4 11\sigma^1 1\delta^2$ ($^4\Sigma^-$), and (core)$9\sigma^1 1\delta^2 4\pi^2$ ($^6\Sigma^-$).[19−21] It is perhaps correct to assume that a similar case holds for VCl^+, and thus the $^4\Sigma^-$ state is formed from a $11\sigma^1 5\pi^2$ configuration. A $11\sigma^1 1\delta^2$ configuration would also generate a $^4\Sigma^-$ state, as in the case of VO and VS.[5,9] The $11\sigma^1 5\pi^2$ and $11\sigma^1 1\delta^2$ configurations are distinguished by the sign of the c hyperfine parameter, which, as discussed later, has a different sign for VCl^+ as opposed to VO, supporting the $\sigma^1\pi^2$ electron configuration.

The fine structure pattern and large value of λ for VCl^+ indicates that the molecule has a case (a) $^4\Sigma^-$ ground state, perhaps best illustrated by the energy level diagram shown in Figure 4. Here the $N = 31$, 32, and 33 energy levels are shown (hyperfine splittings are insignificant on this scale). They are split into the four spin components labeled by F_1 (solid line), F_2 (dashed line), F_3 (dotted line), and F_4 (dot-dashed line). The fine structure levels are separated into effective Ω ladders with the F_1 and F_4 components corresponding to $\Omega = \pm^1/_2$ at lower energy, and the F_2 and F_3 levels correlated with $\Omega = \pm^3/_2$ at higher energy. The F_2 and F_3 components are in fact nearly degenerate at the same value of J. (The separation between these two components has been exaggerated on the scale of this figure.)

The large values of γ and λ indicate a considerable degree of second-order spin−orbit coupling, as is common for heavy molecules. The spin−spin parameter λ is a sum of the pure microscopic electron spin-nuclear rotation coupling and the second-order spin−orbit effect, i.e., $\lambda = \lambda^{ss} + \lambda^{so}$.[27] The second-order term arises from interactions with a nearby $^2\Sigma^+$ state that is isoconfigurational with the ground $^4\Sigma^-$ state. The energy of this excited state, assuming the single-perturber approximation, can be calculated from λ^{so} using the following equation:[10]

$$\lambda^{so} = \frac{1}{4}\frac{|\langle^2\Sigma^+|\hat{H}_{SO}|X^4\Sigma^-_{1/2}\rangle|^2}{E(^2\Sigma^+) - E(X^4\Sigma^-)} \quad (2)$$

The expression simplifies to

$$\lambda^{so} \approx \frac{1}{6}\frac{a_{3d}{}^2}{E(^2\Sigma^+) - E(X^4\Sigma^-)} \quad (3)$$

where a_{3d} is the spin−orbit constant for V^{2+}. Using $a_{3d} = 167$ cm^{-1} and letting $\lambda \sim \lambda^{so}$,[27] then the energy of the $^2\Sigma^+$ state is estimated to be ∼333 cm^{-1}. This energy is much lower in VCl^+ than for the corresponding states in VO or VS, which have $\Delta E \sim 10\,000$ cm^{-1}.[5,11]

The spin-rotation parameter γ is also a sum of the first order spin-rotation coupling and the second-order spin−orbit effect, i.e., $\gamma = \gamma^{sr} + \gamma^{so}$.[27] The selection rule for the latter interaction is $\Delta S = 0$; therefore, in analogy to VO and VS, γ^{so} arises from perturbations by a nearby $^4\Pi$ state (or states).[5,11] If the single-perturber approximation is assumed and $\gamma \sim \gamma^{so}$, then the energy of the nearest $^4\Pi$ state can be calculated from γ as follows:[28]

$$\gamma^{so} = \frac{2}{\sqrt{3}}\frac{\langle^4\Pi|AL_+|X^4\Sigma^-\rangle\langle^4\Pi|BL_+|X^4\Sigma^-\rangle}{E(^4\Pi) - E(X^4\Sigma^-)} \quad (4)$$

Assuming the $A \sim a_{3d}(V^{2+})$, then eq 4 reduces to

$$\gamma^{so} = \frac{4}{3}\frac{B_0 a_{3d}}{E(^4\Pi) - E(X^4\Sigma^-)} \quad (5)$$

From this equation, the energy of the $^4\Pi$ state is established to be ∼184 cm^{-1}. In comparison, the one theory paper on VCl^+ predicts a $^4\Sigma - {}^4\Pi$ separation of 520 cm^{-1}, but with the $^4\Pi$ state lower in energy.[22] The corresponding energies in VO and VS are ∼9500 and ∼3500 cm^{-1}.[11,29] Although these calculations involve numerous assumptions, they suggest that the density of low-lying excited electronic states is greater in VCl^+ than in either VO or VS.

The presence of close-by excited states is also apparent in the large magnitudes of γ_s and b_s: 1436(51) MHz and −96.1(7.6) MHz, respectively. Both terms are usually less than 1 MHz, as seen in MnO and VO.[9,12] These constants are third-order

parameters involving cross terms between spin−orbit coupling and the first-order spin-rotation (γ_s) or Fermi contact interactions (b_s). In analogy to γ and λ, these parameters are related to the energies of perturbing $^4\Pi$ and $^2\Sigma$ electronic states.[25,26]

The large value of b_s additionally produces the dissimilar hyperfine patterns between the F_1 and F_4 relative to F_2 and F_3 spin components, as seen in Figure 2. Cheung and Merer note that b_s essentially creates an effective b parameter of $b_{eff} \cong b_F - {}^1/_2 b_s$ for the F_1 and F_4 levels, and $b_{eff} \cong b_F + {}^9/_2 b_s$ for the F_2 and F_3 levels.[26] This effective constant would normally only cause a negligible difference in the hyperfine energies because b_s is usually much smaller than b_F.[9,12] For VCl^+, however, b_s is comparable to b_F, leading to $b_{eff} \cong 186$ MHz for the F_1 and F_4 components and $b_{eff} \cong -294$ MHz for the other two components. The differing signs of b_{eff} also explain the reversal in the ordering of the hyperfine components in the F_1 and F_4 levels compared to the F_2 and F_3 spin states, as discussed previously.

The Fermi contact term b_F arises from unpaired electrons in the sσ orbitals. The value of this constant in VCl^+ is 138(14) MHz. The $\sigma^1\pi^2$ configuration is assumed to arise from exclusively 3d electrons. In this case, $b_F = 0$. However, as noted by Bridgman and Rothery,[30] usually there is sdσ hybridization in the 3d metals as they form molecules. The positive, nonzero Fermi contact term for VCl^+ indicates that such hybridization must be occurring.

The dipolar constant c is positive and large ($c = 341(63)$ MHz). In contrast, the values of c for VO and VS are $-129.84(19)$ and $-78(12)$,[5,9] i.e., smaller and negative. The parameter c is related to the expectation values of the quantity $\sum_i (3\cos^2\theta_i - 1)/r^3$ for p and d electrons. The negative values for c in VO and VS are explained by the $\sigma^1\delta^2$ configuration in these species. The $(3\cos^2\theta - 1)$ term for dδ electrons is negative, $-{}^4/_7$,[13] resulting in negative c values. The term for dπ electrons is ${}^2/_7$.[13] Hence, qualitatively, the difference in signs reflects the variation in electron configuration, $\sigma^1\delta^2$ vs $\sigma^1\pi^2$. Using c for VCl^+, the quantity $\langle 1/r^3\rangle$ is estimated to be 2.87×10^{25} cm^{-3}, similar in magnitude to that calculated for MnH.[13]

The electric quadrupole constant eQq in VCl^+ arises from interactions of the quadrupole moment of ^{51}V with the electric field gradient caused by both unpaired 3dπ and 3dσ electrons, and the paired valence electrons. The contribution to this parameter from the unpaired electrons can be estimated using the radial and the angular expectation values, $\langle 1/r^3\rangle$ and $(3\cos^2\theta - 1)$, as given above, as well as the angular factor for 3dσ electrons of ${}^4/_7$ and the quadrupole moment of ^{51}V, -0.052×10^{-24} cm^2,[31] and the following equation:

$$eQq = -e^2Q\sum_i \left\langle \frac{3\cos^2\theta_i - 1}{r_i^3} \right\rangle_i \qquad (6)$$

From this expression, eQq is estimated to be 59 MHz. The observed parameter is $-560(180)$ MHz for $V^{35}Cl^+$; see Table 2. The difference between these two numbers suggests that the polarization of the paired bonding valence electrons contributes significantly to the quadrupole interaction. A similar effect is observed in other 3d species, such as MnO and TiO.[12,32]

The V−Cl bond lengths calculated from the rotational constants of $V^{35}Cl^+$ and $V^{37}Cl^+$ are $r_0 = 2.119173(2)$ Å and 2.118988(4) Å. The difference in the distance between the two isotopologues is 0.0002 Å. The average bond length is 2.119 Å, close to the theoretical estimate of 2.16 Å.[22] The value is also 0.100 Å shorter than that in VCl, where $r_0 = 2.219$ Å.[3] As in $TiCl^+$ and TiF^+,[18,19] the metal−halide bond length shortens in the ionic species relative to the neutral molecule. This property is thought to result from the increase in the effective nuclear charge of the metal, which causes the orbitals to contract in the ionic case. This trend is illustrated in Figure 5, which shows a graph of the bond lengths for the 3d transition metal chlorides MCl and MCl^+. Furthermore, this effect is larger for VCl^+ (0.100 Å) than $TiCl^+$ (0.079 Å).[19]

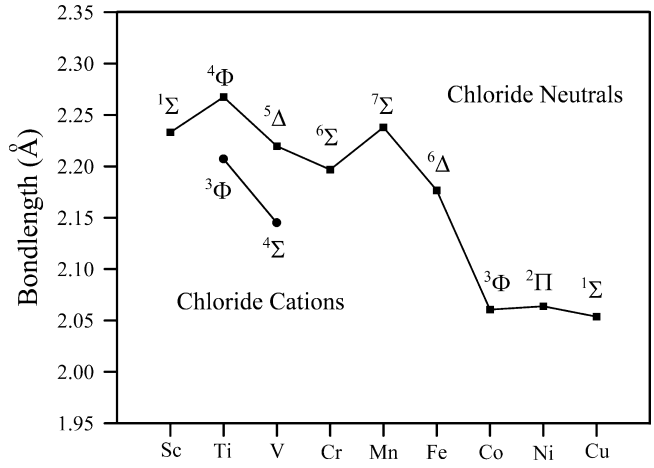

Figure 5. Graph showing the periodic trend in bond lengths for the 3d transition metal chloride neutrals and corresponding cations. The chloride cations have shorter bond lengths than their neutral counterparts by a significant amount. The shortening of the bond distance is thought to be due to an increase in the electrostatic attraction in the cation species. It is unclear whether this trend continues over the complete 3d series.

Not all neutral/ionic pairs show this decrease. For the FeCO/$FeCO^+$ pair, for example, the metal−ligand bond length increases in $FeCO^+$ by ∼0.13 Å.[21] This change is interpreted as the loss of an electron in a bonding orbital. For the FeO/FeO^+ combination, the electron is lost from a nonbonding δ orbital. As a result, only a small increase (0.02 Å) in the bond length is found.[20] These species are obviously more covalent than the 3d halide species and orbital occupancy dominates the bond distances.

6. Conclusion

This study of the pure rotational spectrum of VCl^+ has established the ground state term to be $^4\Sigma^-$ with the likely electron configuration $\sigma^1\pi^2$. This configuration results from the removal of the single δ electron from the orbitals of VCl. Both the spectra and resulting constants suggest that several excited states lie very close in energy to the ground state. The bond lengths of the known metal chloride ions, $TiCl^+$ and VCl^+, are shorter than their neutral counterparts, speculated to be a byproduct of the increased positive charge on the molecule. Investigation of additional metal-containing chloride ions MCl^+ will provide further insight into the bonding of these species.

Acknowledgment. We thank A. J. Merer for suggestions in the analysis of these spectra. This research is supported by NSF grant CHE 07-18699 and NASA grant NNX06AB64G.

Supporting Information Available: Table of observed rotational transitions. This material is available free of charge via the Internet at http://pubs.acs.org.

References and Notes

(1) Halfen, D. T.; Ziurys, L. M. *Astrophys. J.* **2008**, *672*, L77.
(2) Ram, R. S.; Liéven, J.; Bernath, P. F.; Davis, S. P. *J. Mol. Spectrosc.* **2003**, *217*, 186.

(3) Halfen, D. T.; Ziurys, L. M.; Brown, J. M. *J. Chem. Phys.* **2009**, *130*, 164301.
(4) Maeda, A.; Hirao, T.; Bernath, P. F.; Amano, T. *J. Mol. Spectrosc.* **2001**, *210*, 250.
(5) Ran, Q.; Tam, W. S.; Cheung, A.S.-C.; Merer, A. J. *J. Mol. Spectrosc.* **2003**, *220*, 87.
(6) Sheridan, P. M.; Brewster, M. A.; Ziurys, L. M. *Astrophys. J.* **2002**, *576*, 1108.
(7) Tanaka, K.; Shirasaka, M.; Tanaka, T. *J. Chem. Phys.* **1997**, *106*, 6820.
(8) Allen, M. D.; Ziurys, L. M.; Brown, J. M. *Chem. Phys. Lett.* **1996**, *257*, 130.
(9) Flory, M. A.; Ziurys, L. M. *J. Mol. Spectrosc.* **2008**, *247*, 76.
(10) Cheval, G.; Femenias, J.-L.; Merer, A. J.; Sassenberg, U. *J. Mol. Spectrosc.* **1988**, *131*, 113.
(11) Cheung, A. S.-C.; Hansen, R. C.; Merer, A. J. *J. Mol. Spectrosc.* **1982**, *91*, 165.
(12) Namiki, K.; Saito, S. *J. Chem. Phys.* **1997**, *107*, 8848.
(13) Varberg, T. D.; Field, R. W.; Merer, A. J. *J. Chem. Phys.* **1991**, *95*, 1563.
(14) Focsa, C.; Pinchemel, B.; Collet, D.; Huet, T. R. *J. Mol. Spectrosc.* **1998**, *189*, 254.
(15) Focsa, C.; Pinchemel, B.; Femenias, J.-L.; Huet, T. R. *J. Chem. Phys.* **1997**, *107*, 10365.
(16) Zhou, M.; Andrews, L. *J. Chem. Phys.* **1999**, *110*, 10370.
(17) Aguirre, F.; Husband, J.; Thompson, C. J.; Stringer, K. L.; Metz, R. B. *J. Chem. Phys.* **2003**, *119*, 10194.
(18) Halfen, D. T.; Ziurys, L. M. *J. Mol. Spectrosc.* **2006**, *240*, 58.
(19) Halfen, D. T.; Ziurys, L. M. *J. Mol. Spectrosc.* **2005**, *234*, 34.
(20) Halfen, D. T.; Ziurys, L. M. Manuscript in preparation.
(21) Halfen, D. T.; Ziurys, L. M. *Astrophys. J.* **2007**, *657*, L61.
(22) Kardahakis, S.; Mavridis, A. *J. Phys. Chem. A* **2009**, *113*, 6818.
(23) Savage, C.; Ziurys, L. M. *Rev. Sci. Instrum.* **2005**, *76*, 043106.
(24) Brown, J. M.; Carrington, A. *Rotational Spectroscopy of Diatomic Molecules*; Cambridge University Press: New York, 2003.
(25) Brown, J. M.; Milton, D. J. *Mol. Phys.* **1976**, *31*, 409.
(26) Cheung, A. S.-C.; Merer, A. J. *Mol. Phys.* **1982**, *46*, 111.
(27) Lefebvre-Brion, H.; Field, R. W. *The Spectra and Dynamics of Diatomic Molecules*; Elsevier: Amsterdam, 2004.
(28) Brown, J. M.; Colbourn, E. A.; Watson, J. K. G.; Wayne, F. D. *J. Mol. Spectrosc.* **1979**, *74*, 294.
(29) Cheung, A. S.-C.; Taylor, A. W.; Merer, A. *J. Mol. Spectrosc.* **1982**, *82*, 391.
(30) Bridgeman, A. J.; Rothery, J. *J. Chem. Soc., Dalton Trans.* **2000**, 211.
(31) Raghavan, P. *At. Data Nucl. Data Tables* **1989**, *42*, 189.
(32) Namiki, K.; Saito, S.; Robinson, J. S.; Steimle, T. C. *J. Mol. Spectrosc.* **1998**, *191*, 176.

JP9058142